European Journal of Medicinal Chemistry 65 (2013) 477–486

Contents lists available at SciVerse ScienceDirect

European Journal of Medicinal Chemistry

journal homepage: http://www.elsevier.com/locate/ejmech

Original article

Naphthalimides exhibit *in vitro* antiproliferative and antiangiogenic activities by inhibiting both topoisomerase II (topo II) and receptor tyrosine kinases (RTKs)

Xin Wang [a], Zhuo Chen [a,b,*], Linjiang Tong [b], Shaoying Tan [a], Wei Zhou [a], Ting Peng [b], Kun Han [b], Jian Ding [b], Hua Xie [b,**], Yufang Xu [a,***]

[a] State Key Laboratory of Bioreactor Engineering, Shanghai Key Laboratory of Chemical Biology, Shanghai Key Laboratory of New Drug Design, School of Pharmacy, East China University of Science and Technology, Shanghai 200237, China
[b] Division of Anti-tumor Pharmacology, State Key Laboratory of Drug Research, Shanghai Institute of Materia Medica, Chinese Academy of Sciences, Shanghai 201203, China

ARTICLE INFO

Article history:
Received 28 March 2013
Received in revised form
30 April 2013
Accepted 3 May 2013
Available online 14 May 2013

Keywords:
Angiogenesis
Multitarget
Naphthalimide
Topoisomerase II
Tyrosine kinase

ABSTRACT

Novel naphthalimide derivatives were designed and synthesized to modulate both topoisomerase II (topo II) and receptor tyrosine kinases (RTKs). Most target compounds exhibited effective and selective antiproliferative activities against three cancer cell lines by inhibiting topo II. The IC_{50} values ranged from 1.5 to 19.1 μM. Moreover, compounds **8d** and **12d** moderately inhibited various angiogenesis-related RTKs, including FGFR1, VEGFR2 and PDGFRα. The representative compound **8d** was then proved to possess antiangiogenic activity, which was evidenced by the inhibition of migration and tube formation activities of HMEC-1 cells. To our knowledge, it is the first time naphthalimides were identified as tyrosine kinases inhibitors (TKIs) besides their conventional cytotoxicity.

1. Introduction

DNA topoisomerase II (topo II) is a kind of nuclear enzyme that modulates the topology of chromosomal DNA by causing transient double-stranded break. The enzyme plays key roles in a number of DNA-related processes [1]. Topo II is frequently overexpressed in different types of tumors, and has been proved as one of the ideal molecular targets for widely prescribed chemotherapy agents [2]. A number of topo II-targeted chemotherapy drugs, such as Etoposide (VP-16), Doxorubicin (DOX) and Mitoxantrone, have been approved by FDA for clinical use [3]. Despite the emergence of kinase inhibitors, topo II inhibitors still make great contributions in clinic for cancer therapy [4].

Receptor tyrosine kinases (RTKs) are primary mediators of the signaling networks that transmit extracellular signals into the cells. They are vital in many cellular processes including proliferation, differentiation, migration and angiogenesis [5,6]. There are more than 20 subfamilies of receptor tyrosine kinases that have been discovered so far, including epidermal growth factor receptor (EGFR) family, vascular endothelial growth factor receptor (VEGFR) family, platelet-derived growth factor receptor (PDGFR) family, fibroblast growth factor receptor (FGFR) family [7]. Aberrant RTKs activities are implicated with tumor growth and development, and thus provide popular targets in cancer therapy [8]. Numerous RTKs inhibitors have been developed and several of them have been approved for clinical use.

Angiogenesis is essential in tumor progression by providing both oxygen and nutrition for tumors beyond the size of 1–2 mm^3 [9]. Antiangiogenesis has been proved to be a promising strategy

Abbreviations: EGFR, epidermal growth factor receptor; FGFR, fibroblast growth factor receptor; HMEC-1, Human Microvascular Endothelial Cells; kDNA, kinetoplast DNA; PDGFR, platelet-derived growth factor receptor; RTK, Receptor Tyrosine Kinase; Topo II, topoisomerase II; TKIs, tyrosine kinases inhibitors; VEGFR, vascular endothelial growth factor receptor.

* Corresponding author. State Key Laboratory of Bioreactor Engineering, Shanghai Key Laboratory of Chemical Biology, Shanghai Key Laboratory of New Drug Design, School of Pharmacy, East China University of Science and Technology, Shanghai 200237, China. Tel./fax: +86 21 64250823.
** Corresponding author. Tel.: +86 21 50805897; fax: +86 21 50806722.
*** Corresponding author. Tel.: +86 21 64251399; fax: +86 21 64252603.
E-mail addresses: chenzhuo@ecust.edu.cn (Z. Chen), hxie@simm.ac.cn (H. Xie), yfxu@ecust.edu.cn (Y. Xu).

0223-5234/$ – see front matter © 2013 Elsevier Masson SAS. All rights reserved.
http://dx.doi.org/10.1016/j.ejmech.2013.05.002

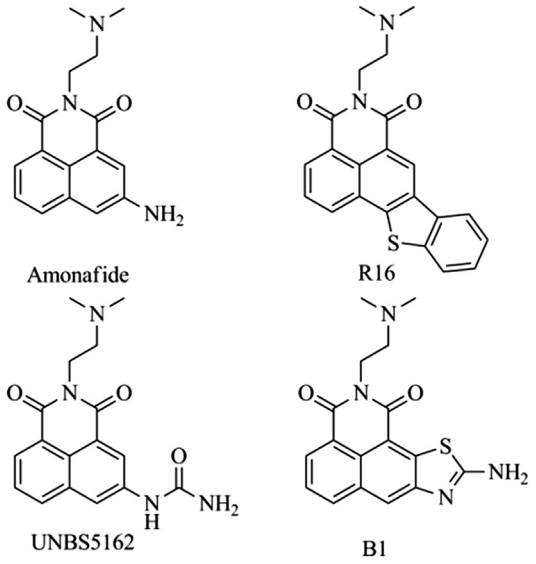

Fig. 1. Representative compounds of naphthalimides.

for the treatment of cancers with few side effects [10,11]. Many investigations have proved that angiogenesis is regulated by cytokines and specific tyrosine kinases like VEGFR, PDGFR and FGFR [12]. Tyrosine kinases inhibitors (TKIs) which inhibit angiogenesis have been developed for clinical use. For example, the VEGFR and PDGFR inhibitor Sunitinib has been approved in the treatment of renal cell carcinoma which is a highly vascularized tumor [13].

As tumors involve complex biological networks, it is not easy to provide long-term effects by targeting a single target in most patients [14,15]. Therefore, multitarget TKIs are desirable for enhancing antitumor potency and overcoming possible resistance mechanism. Antiangiogenic TKIs in clinical use are frequently multitarget kinase inhibitors, such as Sunitinib and Sorafenib [16]. As antiangiogenesis is generally cytostatic rather than cytoreductive, recent studies have indicated that combination of antiangiogenic agents with cytotoxic chemotherapy agents is more effective in cancer treatment [17]. While direct damage of endothelial cells could improve antiangiogenic effects, the antiangiogenic agents will normalize vessels and improve delivery of cytotoxic drugs to tumor [7]. As combinational therapy used in clinic usually exhibited complex pharmacokinetic and pharmacodynamic relationships and toxicology profiles [18], discovering single agents with both antiangiogenic and cytotoxic activities is a desirable strategy for cancer therapy.

Naphthalimides, first discovered by Brana and co-workers [19], are a class of DNA intercalators showing potent antitumor activities against various cancers preclinically and clinically [20–23]. Amonafide is one of the most active naphthlimide-based topo II poisons and is in phase III clinical trials for the treatment of acute myeloid leukemia. Heterocyclic fused naphthalimides and bisnaphthalimides showed great DNA binding affinity and cytotoxic activity. Several of them also entered clinical trials [20,24]. Besides modulating DNA-related processes, new mechanisms of action have been verified for naphthalimide skeleton, which suggests novel therapeutic strategies with naphthalimide derivatives. For example, UNBS5162 could depress expression of the chemokines, and induce antiangiogenic effects *in vivo* [21].

According to our previous research, some of the naphthalimide derivatives with long alkyl chains and polyamines exhibited more potent antiproliferative activity than Amonafide. For example, compounds **7c** and **7d** could inhibit topo II and induce lysosomal membrane permeabilization (LMP) and apoptosis (see Fig. 1) [25]. Compounds **8d** and **12d** were analogs of **7c** and **7d** with long alkyl chains at 2-position and polyamines at the 6-position. They also showed potent antiproliferative activity by inhibiting topo II. Herein, we designed and synthesized the derivatives of **8d** and **12d** with different lengths of alkyl chains. These newly-synthesized compounds inhibited topo II activity and exhibited structure–activity relationship in proliferation of different types of cancer cells. Furthermore, tyrosine kinases were proved to be the antitumor targets of naphthalimide derivatives for the first time. The representative compound **8d** exhibited potent antiangiogenesis activity *in vitro*.

2. Results and discussions

2.1. Chemistry

As shown in Scheme 1, the target compounds **1d**–**16d** were prepared in a facile four-step sequence with good yields [25]. Commercially available 6-bromobenzo[de]-isochromene-1,3-dione was condensed with corresponding amines to yield **1a**–**16a**, which were converted to **1b**–**16b** under Ullmann's condition. The alcohol were then converted to the corresponding bromides **1c**–**16c** using a system of Ph_3P, 2,3-dichloro-5,6-dicyano-benzoquinone (DDQ)

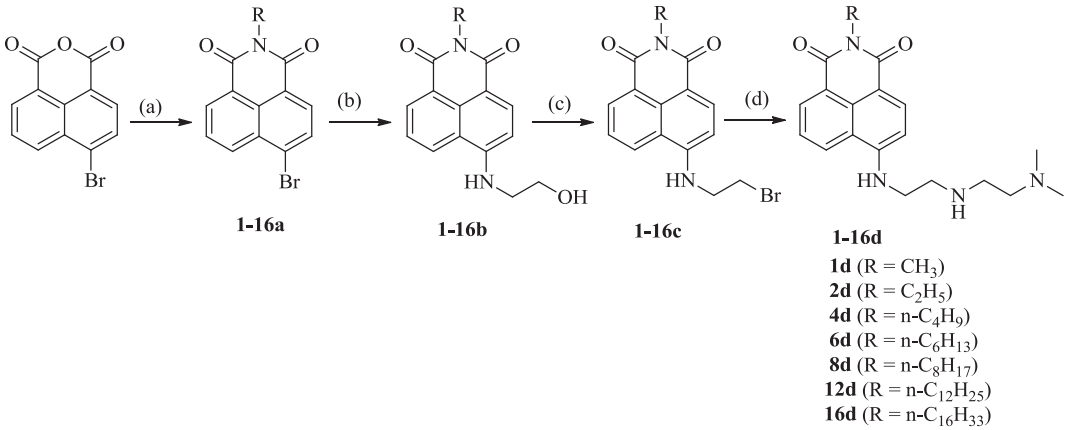

Scheme 1. Reagents and conditions: a) 1.1 equiv of corresponding primary amines, ethanol, reflux, yield 81–95%, (for **1a** and **2a** corresponding 70% amines aqueous were used as solvent, and reacted at r.t., yield 90–95%); b) 3.0 equiv of ethanolamine, 2-methoxyethanol, reflux, yield 72–88%; c) 1.2 equiv of DDQ, 1.2 equiv of PPh_3, 1.2 equiv of (n-butyl)$_4$NBr, CH_2Cl_2, r.t., yield 78–83%; d) 5.0 equiv of polyamines, 1.2 equiv of KI, $CHCl_3$, reflux, yield 62–71%.

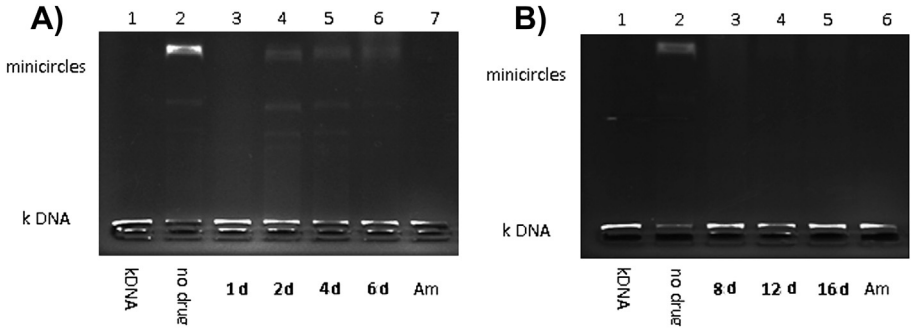

Fig. 2. Inhibition of topo II-mediated kDNA decatenation by target compounds (100 μM). (A) Lane 1, kDNA; lane 2, minicircles (no drug); lanes 3–7, compounds **1d**, **2d**, **4d**, **6d** and Amonafide, respectively. (B) Lane 1, kDNA; lane 2, minicircles (no drug); lanes 3–6, compounds **8d**, **12d**, **16d**, and Amonafide, respectively.

and tetrabutyl ammonium bromide [26]. Finally, the reactions between **1c**–**16c** and N′,N′-dimethylethane-1,2-diamine were accomplished in chloroform to provide the target compounds **1d**–**16d**.

2.2. Topo II inhibition

As naphthalimides could inhibit the activity of topo II by forming a complex of drug-DNA-topoisomerase [27,28], the kinetoplast DNA (kDNA) decatenation assay was taken to investigate the topo II inhibitory effect in cell-free system [29]. As illustrated in Fig. 2, topo II catalyzed the decatenation of kDNA to minicircles in the presence of ATP (lane 2 vs. lane 1). All the tested compounds could reduce the kDNA minicircles, which indicated their topo II inhibition capacity. The images were quantitated by software Gel-Pro Analyzer (Fig. S1 and Table S1). Compounds **1d** and **6d**–**16d** exhibited similar topo II inhibitory potency as Amonafide at the tested concentration. Meanwhile, compounds **2d** and **4d** were less potent topo II inhibitors in comparison with Amonafide.

2.3. In vitro antiproliferative activity

The antiproliferative activity of compounds **1d**–**16d** was evaluated against three human cancer cell lines and two normal cell lines: HL-60 (human promyelocytic leukemia cell line), MDA-MB-231 (human breast cancer line), A549 (human lung adenocarcinoma epithelial cell line), LO2 (human liver cell line) and GES-1 (human gastric epithelial mucosa cell line).

As shown in Table 1, the length of alkyl chains significantly influenced the antiproliferative activities. Compounds **6d**–**12d** exhibited significant antitumor activity with IC_{50} values mainly at single digital micromolar range, which were comparable with the reference compound Amonafide. These results were in accordance with their potent topo II inhibitory activity and balanced solubility and membrane penetrability (see Table 1). Whereas, compounds **1d**–**4d** and **16d** showed much weaker antiproliferative activity with IC_{50} values mainly at double digit micromolar. The less potent antitumor activity of **2d** and **4d** might be owing to their weaker topo II inhibitory potency, while poor membrane penetrability of **1d** and poor aqueous solubility of **16d** might underlie their weaker antiproliferative activities (see Table 1). Besides, the tested compounds did not intercalate in ct-DNA as effectively as conventional naphthalimide derivative according to CD spectra and fluorescent spectra studies (Fig. S2 and S3). We further investigated the antiproliferative effect on normal cell lines-LO2 and GES-1. In comparison with tumour cell lines, less cytotoxicity was observed on normal cells, with IC_{50} values mainly higher than 50 μM. Therefore, the target compounds exhibited good selectivity against tumor cell lines.

2.4. RTK inhibition

According to recent reports, the naphthalimides can modulate AKT/mTOR signaling pathway [30,31]. As AKT/mTOR is one of the representative downstream signal pathways of tyrosine kinases, we assumed that naphthalimides might target tyrosine kinases and thereby down-regulate AKT/mTOR pathway. We investigated the tyrosine kinases inhibition activity of the derivatives using ELISA method. As shown in Table 2, **8d** inhibited FGFR1 and KDR (VEGFR2) kinase activities with IC_{50} at 18.06 and 48.94 μM respectively. **12d** also inhibited FGFR1 and KDR at micromolar range. Besides, **12d** inhibited PDGFRα with IC_{50} value at 26.17 μM. Their analogs exhibited no inhibition activity against the tested kinases at the concentration of 50 μM or higher. Though the kinases inhibition activity of these compounds was still much weaker than

Table 1
Antiproliferative activities and physical properties of compounds **1d**–**16d**.

No.	Antiproliferative activities (IC_{50}, μM)					Physical properties	
	HL60	MDA-MB-231	A549	LO2	GES-1	Solubility (μM)	LogP
1d	7.8 ± 1.0	7.9 ± 1.0	24.5 ± 5.6	13.6 ± 0.7	>50	78.4 ± 1.9E3	0.15
2d	17.0 ± 1.1	24.3 ± 3.2	31.4 ± 7.0	>50	>50	46.7 ± 5.0E3	0.68
4d	5.8 ± 0.3	10.5 ± 0.9	21.4 ± 8.1	>50	>50	15.4 ± 2.5E3	1.74
6d	1.5 ± 0.5	6.1 ± 0.2	9.8 ± 4.0	>50	46.0 ± 3.5	430 ± 20	2.80
8d	2.1 ± 0.4	8.6 ± 1.8	7.8 ± 1.2	>50	>50	264 ± 13	3.86
12d	1.8 ± 0.2	6.6 ± 2.2	19.1 ± 7.6	>50	>50	63 ± 7	5.99
16d	24.5 ± 8.0	17.7 ± 1.1	31.3 ± 2.0	>50	>50	16 ± 2	8.12
Am	0.9 ± 0.3	4.4 ± 1.0	3.2 ± 1.8	13.8 ± 1.0	21.6 ± 1.6	ND[a]	ND

[a] ND: not determined.

Table 2
Receptor tyrosine inhibition of the target compounds **1d**–**16d**.

Compd.	IC_{50} (μM)			
	KDR	PDGFRα	PDGFRβ	FGFR1
1d	>100	>100	>100	>100
2d	>100	>100	>100	>100
4d	>100	>100	>100	>100
6d	>100	>100	>100	>100
8d	48.94 ± 0.41	>100	>50	18.06 ± 2.42
12d	27.64 ± 0.93	26.17 ± 2.67	>50	28.79 ± 7.52
16d	>100	>50	>50	>100
BIBF1120	<0.001	0.004	0.002	0.060

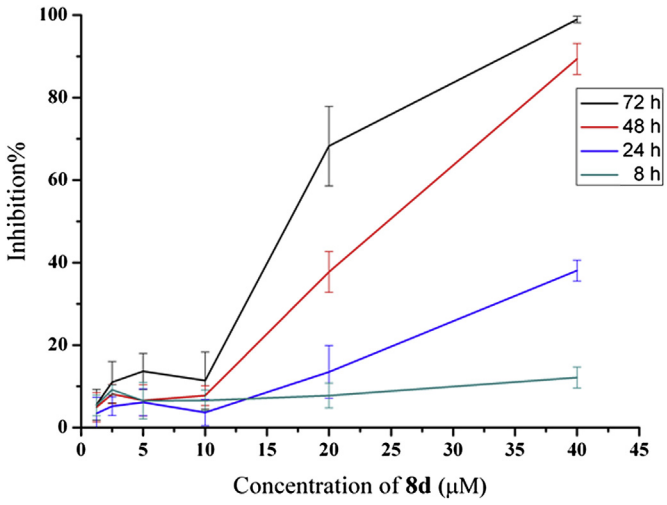

Fig. 3. The antiproliferative activity of **8d** on HMEC-1endothelial cells.

BIBF1120, a multitarget kinase inhibitor in clinical trial, it is the first time naphthalimides were verified to be tyrosine kinase inhibitors.

2.5. Antiangiogenic activity of compound **8d**

Angiogenesis is a complex process which includes the proliferation, migration and tube formation of endothelial cells [32]. As KDR, FGFR1 and PDGFR are highly related with angiogenesis process, we evaluated antiangiogenic activity of **8d** which exhibited more balanced solubility and penetration activity than **12d**, by examining migration and tube formation activities of human microvascular endothelial cells (HMEC-1).

2.5.1. Inhibition of proliferation of HMEC-1

We first examined the growth inhibition effect of compound **8d** on HMEC-1 cells by SRB assay. We found that treatment with compound **8d** for 72 h at the concentrations of 20 μM and 40 μM caused a dose-dependent inhibition of HMEC-1 cell proliferation. As shown in Fig. 3, after 72 h treatment, compound **8d** could inhibit around 68% and 99% cell proliferation at 20 μM and 40 μM, respectively, while 10 μM or lower concentrations of **8d** did not induce appreciable changes in cell growth. Subsequently, **8d** was used in the following antiangiogenesis assay with highest concentration at 10 μM.

2.5.2. Inhibition of migration

Endothelial cell migration, which occurs through chemotaxis, is necessary for angiogenesis. To investigate the effect of **8d** on the migration of HMEC-1 cells *in vitro*, a transwell Boyden chamber assay was performed. We found that treatment with **8d** for 6 h could reduce the number of migrated cells in a dose-dependent manner. As illustrated in Fig. 4A, after exposed to 5 μM of **8d**, about 55% of the migrated HMEC-1 cells were inhibited. Moreover,

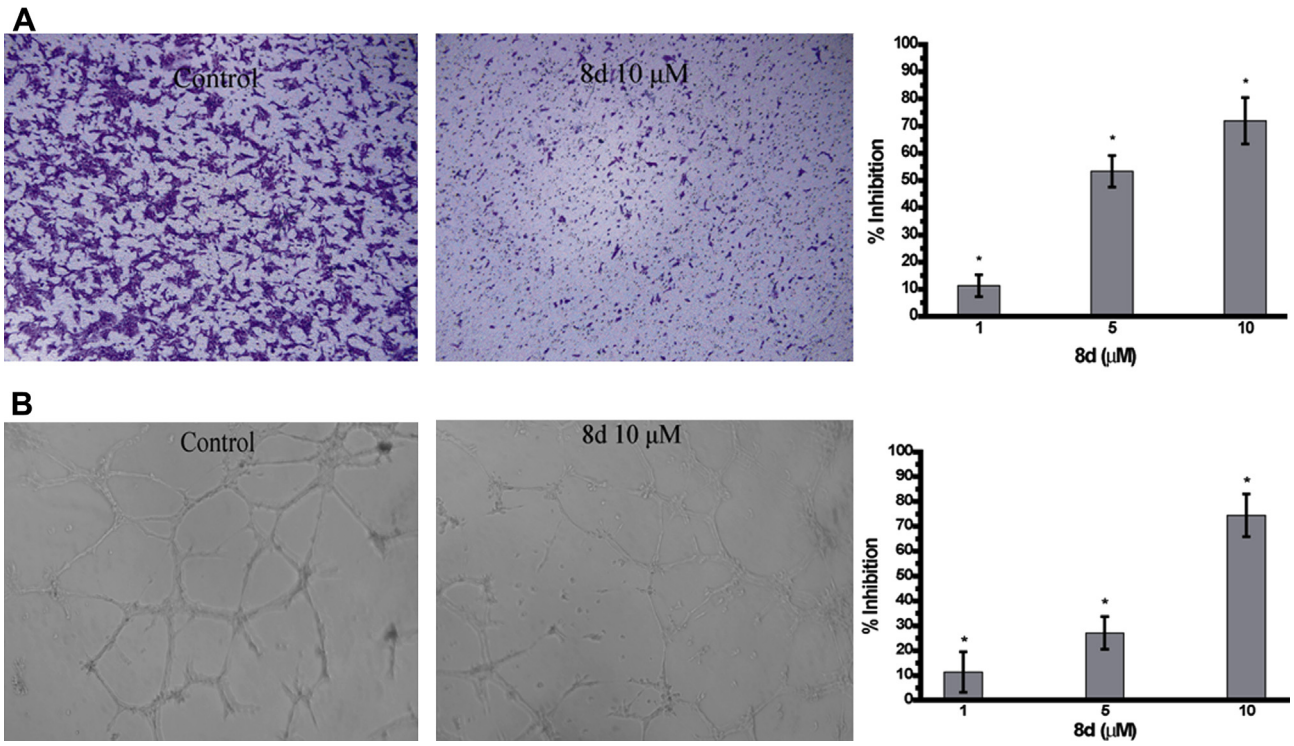

Fig. 4. Inhibitory effect of **8d** on HMEC-1 cells migration and tube formation activities. (A) Representative images and summary data (bar graphs on right hand side) showing inhibition of migration; (B) Representative images and summary data (bar graphs on right hand side) showing inhibition of migration tube formation. Results are expressed as mean ± SD; $n = 3$; $^*P < 0.01$ vs. control.

70% of cell migration was inhibited when the concentration reached 10 μM.

2.5.3. Inhibition of tube formation

Tube formation is one of the most important traits of endothelial cells on matrigel substratum. To further characterize the anti-angiogenesis activity of **8d**, we investigated the inhibitory effect of the formation of functional tubes by plating HMEC-1 cells on matrigel substratum. As shown in Fig. 4B, in the control group, stimulation of 20% serum resulted in a rapid alignment of HMEC-1s and formation of tube-like structures within 8 h. Compound **8d** could effectively inhibit serum-stimulated tube formation of HMEC-1 cells in a dose-dependent manner. Treatment with 5 and 10 μM **8d** could induce 30% and 70% inhibition of tube-like structures respectively.

2.6. Down-regulation of FGFR1 phosphorylation and downstream signaling pathways by compound *8d*

We further evaluated the effect of **8d** on the phosphorylation of FGFR1 and its downstream signaling pathways in HMEC-1 cells [33]. Serum-starved HMEC-1 cells were treated with different concentrations of **8d** for 10 h, followed by the addition of 50 ng mL^{-1} bFGF (10 min), then assayed by Western blotting. The results showed that **8d** treatment resulted in a dose-dependent inhibition of FGFR1 phosphorylation induced by bFGF. As shown in Fig. 5, phospho-FGFR1 expression declined after exposure to 1.25 and 2.5 μM **8d** and became undetectable at exposure to 5 μM **8d**. Moreover, the phosphorylation of the key molecules downstream of FGFR, including AKT and Erk, were obviously decreased. Together with the data described above, we concluded that **8d** inhibited angiogenesis by blocking the activation of tyrosine kinases and subsequent downstream signaling.

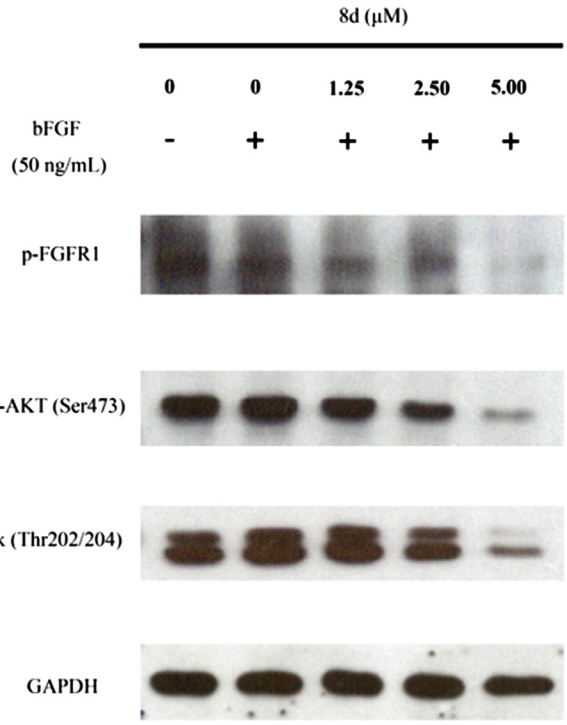

Fig. 5. **8d** down-regulated the phosphorylation FGFR1 (Tyr 653/654) and downstream Erk1/2 (Thr 202/204) and AKT (Ser 473) signaling pathways induced by bFGF in HMEC-1 cells.

3. Conclusion

In this study, we designed and synthesized a series of naphthalimides with different lengths of alkyl chains and examined their antitumor activity *in vitro*. Compounds **1d**, **6d**–**16d** could inhibit topo II activity as potent as Amonafide in kDNA decatenation assay. In accordance with their topo II inhibition activity, compounds **6d**–**12d** inhibited the growth of cancer cell lines comparably with Amonafide. Besides, compounds **1d** and **16d** exhibited less potent anti-proliferative activity because of their poor membrane penetration or aqueous solubility. Meanwhile, the compounds displayed good selectivity to tumour cell lines comparing with normal cell lines.

We further proved that compounds **8d** and **12d** were moderate RTK inhibitors against angiogenesis-related FGFR1, KDR and PDGFRα. To our knowledge, this is the first time naphthalimides were reported as TKIs. We evaluated the antiangiogenesis activity of compound **8d** by investigating the inhibition of proliferation, migration and tube formation of endothelial cells. Compound **8d** could inhibit HMEC-1 cell proliferation at high concentrations (>10 μM) after 72 h treatment. Besides, compound **8d** could significantly inhibit HMEC-1 cells migration and tube formation activities at low concentrations (less than 10 μM) after 6–8 h exposure. Moreover, we proved that the phosphorylation of FGFR1 induced by bFGF, and the phosphorylation FGFR downstream molecules AKT and Erk could be inhibited by **8d** treatment. According to the desirable results, compound **8d** exhibited effective anti-proliferative and antiangiogenic activities by targeting topo II and tyrosine kinases. In all, we provided evidence for further investigation of naphthalimides as multitarget antitumor candidates.

4. Experimental section

All chemical reagents and solvents were purchased from commercial sources and used without further purification. Thin-layer chromatography (TLC) was performed on silica gel plates. Column chromatography was performed using silica gel (Hailang, Qingdao) 300–400 mesh. Biological agents: SRB, MTT and so on were purchased from Sigma Aldrich (St. Louis, MO, USA); all medium and FBS from Gibco (Grand Island, NY, USA); bFGF from R&D systems (Minneapolis, MN, USA); Matrigel from BD Biosciences (San Jose, CA, USA); antibodies to phosphorylated form of the FGF receptor FGFR1, Erk and AKT from Cell Signalling Technology (Danvers, MA, USA); antibody to GAPDH (glyceraldehyde-3-phosphate dehydrogenase) from KangChen Bio-tech (Shanghai); secondary antibodies from Calbiochem (San Diego, CA, USA). The melt points were tested by WRS-1B-digital melting point apparatus. ^{1}H and ^{13}C NMR spectra were recorded employing a Bruker AV-400 spectrometer with chemical shifts expressed in parts per million. The mass spectra were collected at the Mass Instrumentation Facility of the Analysis and Research Center of ECUST. The purities of **1d**–**16d** were analyzed by HPLC, with the purity all being higher than 95% (Table S2). Analytical HPLC was performed on a Hewlett–Packard 1100 system chromatograph equipped with photodiode array detector using a Zorbax Bonus-RP 5 μM 250 mm × 4.6 mm column (reverse phase) to detect the purity of the products. The mobile phase was a gradient of 70–100% methanol (solvent 1) and 10 mM NH_4OAc in water (pH 6.0) (solvent 2) at a flow rate of 1.0 mL/min (0–1.0 min, 0–70% solvent 1; 1.0–15.0 min, 70% solvent 1; 15.0–25.0 min, 70–100% solvent 1).

4.1. Synthesis

*4.1.1. General procedure for the preparation of **1a** and **2a***

To a solution of corresponding 70% amine aqueous, bromobenzo [de]- isochromene-1,3-dione (2.00 g, 7.94 mmol) was added.

The mixture was stirred overnight at room temperature. After completion, the solid was filtered and washed with water and dried in infra-ray oven. Then the product was purified by column chromatography on silica gel (PE:EA = 10:1, v/v) to provide **1a** and **2a**.

*4.1.1.1. 6-Bromo-2-methyl-1H-benzo[de]isoquinoline-1,3(2H)-dione (**1a**).* White solid (95.0% yield); mp: 182.4–183.4 °C; ^{1}H NMR (400 MHz, $CDCl_3$): δ 3.57 (s, 3H, C*H*$_3$), 7.86 (t, *J* = 8.4 Hz, 1H, Ar*H*), 8.06 (d, *J* = 7.6 Hz, 1H, Ar*H*), 8.44 (d, *J* = 8.0 Hz, 1H, Ar*H*), 8.59 (d, *J* = 8.4 Hz, 1H, Ar*H*), 8.68 (d, *J* = 7.2 Hz, 1H, Ar*H*); MS (EI) calcd for $C_{13}H_8BrNO_2$ $[M]^+$: 289.0, found: 289.0.

*4.1.1.2. 6-Bromo-2-ethyl-1H-benzo[de]isoquinoline-1,3(2H)-dione (**2a**).* White solid, (90.2% yield); mp: 164.5–164.7 °C; ^{1}H NMR (400 MHz, $CDCl_3$): δ 1.34 (t, *J* = 7.1 Hz, 3H, C*H*$_3$), 4.24 (q, *J* = 7.1 Hz, 2H, C*H*$_2$CH$_3$), 7.85 (dd, J_1 = 7.4 Hz, J_2 = 8.5 Hz, 1H, Ar*H*), 8.04 (d, *J* = 7.9 Hz, 1H, Ar*H*), 8.41 (d, *J* = 7.9 Hz, 1H, Ar*H*), 8.56 (d, *J* = 8.5 Hz, 1H, Ar*H*), 8.66 (d, *J* = 7.4 Hz, 1H, Ar*H*); ^{13}C NMR (100 MHz, $CDCl_3$): δ 13.3 (CH_2CH_3), 35.7 (CH_2CH_3), 122.3 (Ar*C*), 123.2 (Ar*C*), 128.0 (Ar*C*), 128.9 (Ar*C*), 130.2 (Ar*C*), 130.6 (Ar*C*), 131.1 (Ar*C*), 131.9 (Ar*C*), 133.2 (Ar*C*), 163.3 (*C*=O), 163.4(*C*=O); MS (ESI) calcd for $C_{14}H_{11}BrNO_2$ $[M + H]^+$: 304.0, found: 304.1.

*4.1.2. General procedure for preparation of **4a**, **6a**, and **16a***

To a stirred solution of 6-bromobenzo[de]isochromene-1,3-dione (2.00 g, 7.22 mmol) in EtOH (20 mL) was added the corresponding primary amine (7.94 mmol). The resulting mixture was heated and refluxed for 2–10 h and monitored by TLC. After completion, the reaction mixture was cooled to room temperature and concentrated under vacuum. The crude products were washed with EtOH, and then recrystallized from EtOH.

*4.1.2.1. 6-Bromo-2-butyl-1H-benzo[de]isoquinoline-1,3(2H)-dione (**4a**).* White solid (81.3% yield); mp: 104.7–105.4 °C; ^{1}H NMR (400 MHz, $CDCl_3$): δ 0.98 (t, *J* = 7.2 Hz, 3H, C*H*$_3$), 1.40–1.50 (m, 2H, C*H*$_2$CH$_3$), 1.68–1.75 (m, 2H, $CH_2CH_2CH_2CH_3$), 4.17 (t, *J* = 7.2 Hz, 2H, C*H*$_2$CH$_2$CH$_2$CH$_3$), 7.83 (t, *J* = 8.0 Hz, 1H, Ar*H*), 8.02 (d, *J* = 7.6 Hz, 1H, Ar*H*), 8.40 (d, *J* = 7.2 Hz, 1H, Ar*H*), 8.55 (d, *J* = 8.4 Hz, 1H, Ar*H*), 8.64 (d, *J* = 7.2 Hz, 1H, Ar*H*); ^{13}C NMR (100 MHz, $CDCl_3$): δ 13.8 ($C_2H_6CH_3$), 20.3 ($C_2H_4CH_2CH_3$), 30.2 ($CH_2CH_2CH_2CH_3$), 40.4 ($CH_2C_2H_4CH_3$), 122.3 (Ar*C*), 123.2 (Ar*C*), 128.1 (Ar*C*), 128.9 (Ar*C*), 130.1 (Ar*C*), 130.6 (Ar*C*), 131.0 (Ar*C*), 131.2 (Ar*C*), 131.9 (Ar*C*), 133.2 (Ar*C*), 163.6 (*C*=O); MS (EI) calcd for $C_{16}H_{14}BrNO_2$ $[M]^+$: 331.0, found: 331.0.

*4.1.2.2. 6-Bromo-2-hexyl-1H-benzo[de]isoquinoline-1,3(2H)-dione (**6a**).* White solid (84.6% yield); mp: 66.5–66.7 °C; ^{1}H NMR (400 MHz, $CDCl_3$): δ 0.89 (t, *J* = 6.4 Hz, 3H, C*H*$_3$), 1.33–1.43 (m, 6H, $CH_2CH_2C_3H_6CH_3$), 1.68–1.75 (m, 2H, $CH_2CH_2C_3H_6CH_3$), 4.14 (t, *J* = 7.6 Hz, 2H, C*H*$_2$CH$_2$C$_3$H$_6$CH$_3$), 7.80 (t, *J* = 8.0 Hz, 1H, Ar*H*), 7.98 (d, *J* = 8.0 Hz, 1H, Ar*H*), 8.35 (d, *J* = 7.6 Hz, 1H, Ar*H*), 8.49 (d, *J* = 8.4 Hz, 1H, Ar*H*), 8.60 (d, *J* = 7.2 Hz, 1H, Ar*H*); ^{13}C NMR (100 MHz, $CDCl_3$): δ 14.1 ($C_5H_{10}CH_3$), 22.6 ($C_4H_8CH_2CH_3$), 26.8 ($C_3H_6CH_2CH_2CH_3$), 28.0 ($C_2H_4CH_2C_2H_4CH_3$), 31.5 ($CH_2CH_2C_3H_6CH_3$), 40.6 ($CH_2C_4H_8CH_3$), 122.2 (ArC), 123.1 (ArC), 128.0 (ArC), 128.8 (ArC), 130.1 (ArC), 130.5 (ArC), 131.0 (ArC), 131.1 (ArC), 131.9 (ArC), 133.1 (ArC), 163.4 (*C*=O), 163.5 (*C*=O); MS (ESI) calcd for $C_{18}H_{19}BrNO_2$ $[M + H]^+$: 360.1, found: 360.0.

*4.1.2.3. 6-Bromo-2-cetyl-1H-benzo[de]isoquinoline-1,3(2H)-dione (**16a**).* White solid (85.8% yield); mp: 81.2–81.7 °C; ^{1}H NMR (400 MHz, $CDCl_3$): δ 0.80 (t, *J* = 6.4 Hz, 3H, C*H*$_3$), 1.17–1.34 (m, 26H, $CH_2CH_2C_{13}H_{26}CH_3$), 1.61–1.80 (m, 2H, $CH_2CH_2C_{13}H_{26}CH_3$), 4.08 (t, *J* = 7.6 Hz, 2H, C*H*$_2$CH$_2$C$_{13}$H$_{26}$CH$_3$), 7.77 (t, *J* = 7.2 Hz , 1H, Ar*H*), 7.96 (d, *J* = 8.0 Hz, 1H, Ar*H*), 8.33 (d, *J* = 7.6 Hz, 1H, Ar*H*), 8.48 (d, *J* = 8.8 Hz, 1H, Ar*H*), 8.58 (d, *J* = 7.2 Hz, 1H, Ar*H*); ^{13}C NMR (100 MHz, $CDCl_3$): δ 14.1 ($C_{15}H_{30}CH_3$), 22.7 ($C_{14}H_{28}CH_2CH_3$), 27.1 ($C_{13}H_{26}CH_2CH_2CH_3$), 28.1 ($C_2H_4C_{11}H_{22}C_2H_4CH_3$), 29.4 ($C_2H_4C_{11}H_{22}C_2H_4CH_3$), 29.6 ($C_2H_4C_{11}H_{22}C_2H_4CH_3$), 29.7 ($C_2H_4C_{11}H_{22}C_2H_4CH_3$), 31.9 ($CH_2CH_2C_{13}H_{26}CH_3$), 40.6 ($CH_2CH_2C_{11}H_{22}C_2H_4CH_3$), 122.3 (ArC), 123.2 (ArC), 128.0 (ArC), 128.9 (ArC), 130.1 (ArC), 130.5 (ArC), 131.0 (ArC), 131.1 (ArC), 131.9 (ArC), 133.1 (ArC), 163.4 (*C*=O), 163.5 (*C*=O); MS (EI) calcd for $C_{28}H_{38}BrNO_2$ $[M]^+$: 499.2, found: 499.0.

*4.1.3. General procedure for the preparation of **1b**–**16b***

To a stirred solution of the amination intermediate (5.00 mmol) in 2-methoxyethanol (15 mL), ethanolamine (15.00 mmol) was added. The mixture refluxed for 6–12 h and monitored by TLC. After completion, the reaction mixture was cooled to room temperature and concentrated. The residue was further purified.

*4.1.3.1. 6-(2-Hydroxyethylamino)-2-methyl-1H-benzo[de]isoquinoline-1,3 (2H)-dione (**1b**).* The residue was purified by column chromatography on silica gel (DCM:MeOH = 30:1, v/v) to provide **1b**. Yellow solid (88.6% yield); mp: 223.7–224.5 °C; ^{1}H NMR (400 MHz, $CDCl_3$): δ 3.46 (t, *J* = 6.0, 2H, NHC*H*$_2$CH$_2$OH), 3.54 (s, 3H, C*H*$_3$), 3.69 (t, *J* = 6.0, 2H, NHCH$_2$C*H*$_2$OH), 6.81 (d, *J* = 8.4 Hz, 1H, Ar*H*), 7.67 (t, *J* = 8.0 Hz, 1H, Ar*H*), 8.25 (d, *J* = 8.8 Hz, 1H, Ar*H*), 8.43 (d, *J* = 7.2 Hz, 1H, Ar*H*), 8.68 (d, *J* = 8.4 Hz, 1H, Ar*H*); MS (ESI) calcd for $C_{15}H_{13}N_2O_3$ $[M - H]^-$: 269.1, found: 269.1.

*4.1.3.2. 6-(2-Hydroxyethylamino)-2-ethyl-1H-benzo[de]isoquinoline-1,3 (2H)-dione (**2b**).* The residue was purified by column chromatography on silica gel (DCM:MeOH = 30:1, v/v) to provide **2b**. Yellow solid (73.8% yield); mp: 212.9–213.0 °C; ^{1}H NMR (400 MHz, $CDCl_3$): δ 1.34 (t, *J* = 7.2 Hz, 3H, C*H*$_3$), 3.60 (t, *J* = 4.8 Hz, 2H, NHC*H*$_2$CH$_2$OH), 4.10 (t, *J* = 4.8 Hz, 2H, NHCH$_2$C*H*$_2$OH), 4.24 (q, *J* = 7.2 Hz, 2H, C*H*$_2$CH$_3$), 6.76 (d, *J* = 8.4 Hz, 1H, Ar*H*), 7.64 (t, *J* = 8.0 Hz, 1H, Ar*H*), 8.15 (d, *J* = 8.4 Hz, 1H, Ar*H*), 8.46 (d, *J* = 8.4 Hz, 1H, Ar*H*), 8.58 (d, *J* = 7.2 Hz, 1H, Ar*H*); ^{13}C NMR (100 MHz, DMSO-d_6): δ 13.8 (CH_2CH_3), 34.7 (CH_2CH_3), 46.0 (NHCH_2CH_2OH), 59.2 (NCH_2CH_2OH), 104.3 (Ar*C*), 108.1 (Ar*C*), 120.6 (Ar*C*), 122.4 (Ar*C*), 124.7 (Ar*C*), 129.1 (Ar*C*), 129.9 (Ar*C*), 131.1 (Ar*C*), 134.7 (Ar*C*), 151.3 (Ar*C*), 163.2 (*C*=O), 164.0 (*C*=O); MS (ESI) calcd for $C_{16}H_{17}N_2O_3$ $[M + H]^+$: 285.1, found: 285.1.

*4.1.3.3. 6-(2-Hydroxyethylamino)-2-butyl-1H-benzo[de]isoquinoline-1,3 (2H)-dione (**4b**).* The residue was purified by column chromatography on silica gel (DCM:MeOH = 40:1, v/v) to provide **4b**. Yellow solid (82.0% yield); mp: 171.7–172.3 °C; ^{1}H NMR (400 MHz, $CDCl_3$): δ 0.97 (t, *J* = 7.2 Hz, 3H, $CH_2CH_2CH_2CH_3$), 1.40–1.49 (m, 2H, $CH_2CH_2CH_2CH_3$), 1.69–1.74 (m, 2H, $CH_2CH_2CH_2CH_3$), 3.58 (t, *J* = 5.2 Hz, 2H, NHC*H*$_2$CH$_2$OH), 4.07 (t, *J* = 4.8 Hz, 2H, NHCH$_2$C*H*$_2$OH), 4.16 (t, *J* = 7.6, 2H, C*H*$_2$CH$_2$CH$_2$CH$_3$), 6.78 (d, *J* = 8.4 Hz, 1H, Ar*H*), 7.62 (t, *J* = 8.4 Hz, 1H, Ar*H*), 8.15 (d, *J* = 8.4 Hz, 1H, Ar*H*), 8.44 (d, *J* = 8.4 Hz, 1H, Ar*H*), 8.56 (d, *J* = 7.2 Hz, 1H, Ar*H*); ^{13}C NMR (100 MHz, DMSO-d_6): δ 14.2 ($C_3H_6CH_3$), 20.3 ($C_2H_4CH_2CH_3$), 30.3 ($CH_2CH_2C_2H_5$), 39.4 ($CH_2C_3H_7$), 45.8 (NHCH_2CH_2OH), 59.1 (NCH_2CH_2OH), 104.3 (Ar*C*), 108.1 (Ar*C*), 120.5 (Ar*C*), 122.3 (Ar*C*), 124.7 (Ar*C*), 129.1 (Ar*C*), 129.9 (Ar*C*), 131.2 (Ar*C*), 134.7 (Ar*C*), 151.2 (Ar*C*), 163.4 (*C*=O), 164.2 (*C*=O); MS (ESI) calcd for $C_{18}H_{21}N_2O_3$ $[M + H]^+$: 313.2, found: 313.1.

*4.1.3.4. 6-(2-Hydroxyethylamino)-2-hexyl-1H-benzo[de]isoquinoline-1,3 (2H)-dione (**6b**).* The residue was purified by column chromatography on silica gel (DCM:MeOH = 50:1, v/v) to provide **6b**. Yellow solid (72.4% yield); mp: 146.5–146.8 °C; ^{1}H NMR (400 MHz, $CDCl_3$): δ 0.90 (br, 3H, $CH_2CH_2C_3H_6CH_3$), 1.25–1.42 (m, 6H, $CH_2CH_2C_3H_6CH_3$), 1.69–1.74 (m, 2H, $CH_2CH_2C_3H_6CH_3$), 3.58

(t, J = 4.4 Hz, 2H, NHCH_2CH$_2$OH), 4.07 (t, J = 4.4 Hz, 2H, NHCH$_2$CH_2OH), 4.13 (t, J = 7.6 Hz, 2H, CH_2CH$_2$C$_3$H$_6$CH$_3$), 6.70 (d, J = 8.4 Hz, 1H, ArH), 7.58 (t, J = 7.6 Hz, 1H, ArH), 8.10 (d, J = 8.0 Hz, 1H, ArH), 8.40 (d, J = 8.4 Hz, 1H, ArH), 8.53 (d, J = 7.2 Hz, 1H, ArH); ^{13}C NMR (100 MHz, DMSO-d_6): δ 14.4 (C$_5$H$_{10}$CH$_3$), 22.5 (C$_4$H$_8$CH$_2$CH$_3$), 26.7 (C$_3$H$_6$CH$_2$C$_2$H$_5$), 28.1 (C$_2$H$_4$CH$_2$C$_3$H$_7$), 31.5 (CH$_2$CH$_2$C$_4$H$_9$), 39.6 (CH$_2$C$_5$H$_{11}$), 46.0 (NHCH$_2$CH$_2$OH), 59.1 (NCH$_2$CH$_2$OH), 104.3 (ArC), 108.1 (ArC), 120.6 (ArC), 122.3 (ArC), 124.7 (ArC), 129.0 (ArC), 129.9 (ArC), 131.1 (ArC), 134.7 (ArC), 151.3 (ArC), 163.3 (C=O), 164.2 (C=O); MS (ESI) calcd for C$_{20}$H$_{25}$N$_2$O$_3$ [M + H]$^+$: 341.2, found: 341.1.

*4.1.3.5. 6-(2-Hydroxyethylamino)-2-cetyl-1H-benzo[de]isoquinoline-1,3 (2H)-dione (**16b**).* The residue was purified by column chromatography on silica gel (DCM:MeOH = 50:1, v/v) to provide **16b**. Yellow solid (86.7% yield); mp: 142.7–143.0 °C; ^{1}H NMR (400 MHz, CDCl$_3$): δ 0.90 (t, J = 6.0 Hz, 3H, CH$_2$CH$_2$C$_{13}$H$_{26}$CH_3), 1.27–1.44 (m, 26H, CH$_2$CH$_2$C$_{13}H_{26}$CH$_3$), 1.70–1.77 (m, 2H, CH$_2$CH_2C$_{13}$H$_{26}$CH$_3$), 3.61 (t, J = 5.2 Hz, 2H, NHCH_2CH$_2$OH), 4.10 (t, J = 5.2 Hz, 2H, NHCH$_2$CH_2OH), 4.17 (t, J = 7.6 Hz, 2H, CH_2CH$_2$C$_{13}$H$_{26}$CH$_3$), 6.86 (br, 1H, ArH), 7.67 (t, J = 8.0 Hz, 1H, ArH), 8.19 (d, J = 8.4 Hz, 1H, ArH), 8.48 (d, J = 8.4 Hz, 1H, ArH), 8.61 (d, J = 7.2 Hz, 1H, ArH); ^{13}C NMR (100 MHz, DMSO-d_6): δ 14.4 (C$_{15}$H$_{30}$CH$_3$), 22.6 (C$_{14}$H$_{28}$CH$_2$CH$_3$), 27.0 (C$_{13}$H$_{26}$CH$_2$C$_2$H$_5$), 28.1 (C$_{12}$H$_{24}$CH$_2$C$_3$H$_7$), 29.1 (C$_2$H$_4$C$_{11}$H$_{22}$C$_3$H$_7$), 29.2 (C$_2$H$_4$C$_{11}$H$_{22}$C$_3$H$_7$), 29.3 (C$_2$H$_4$C$_{11}$H$_{22}$C$_3$H$_7$), 29.4 (C$_2$H$_4$C$_{11}$H$_{22}$C$_3$H$_7$), 29.5 (C$_2$H$_4$C$_{11}$H$_{22}$C$_3$H$_7$), 31.8 (CH$_2$CH$_2$C$_{14}$H$_{29}$), 39.6 (CH$_2$C$_{15}$H$_{131}$), 46.0 (NHCH$_2$CH$_2$OH), 59.2 (NCH$_2$CH$_2$OH), 104.3 (ArC), 108.0 (ArC), 120.6 (ArC), 122.3 (ArC), 124.6 (ArC), 129.1 (ArC), 129.9 (ArC), 131.1 (ArC), 134.6 (ArC), 151.3 (ArC), 163.3 (C=O), 164.2 (C=O); MS (ESI) calcd for C$_{30}$H$_{45}$N$_2$O$_3$ [M + H]$^+$: 481.3, found: 481.3.

*4.1.4. General procedure for the preparation of **1c–16c***

To a stirred solution of DDQ (545 mg, 2.40 mmol) and PPh$_3$ (629 mg, 2.40 mmol) in dry CH$_2$Cl$_2$, (n-butyl)$_4$NBr (773 mg, 2.40 mmol) was added at room temperature. **1b–16b** (2.00 mmol) was then added to this mixture, which immediately turned the yellow color of the reaction mixture to deep red. The mixture was stirred at room temperature for 12–24 h. The solvent was then removed under vacuum to fifth of the volume. The residue was purified by column chromatography on silica gel using pure CH$_2$Cl$_2$ as eluant to give the corresponding bromide product.

*4.1.4.1. 6-((2-Bromoethyl)amino)-2-methy-1H-benzo[de]isoquinoline-1,3 (2H)-dione (**1c**).* Orange solid (78.0% yield); mp: 208.8–210.8 °C; ^{1}H NMR (400 MHz, CDCl$_3$): δ 3.54 (s, 3H, CH_3), 3.76 (t, J = 5.8 Hz, 2H, NHCH_2CH$_2$OH), 3.89 (t, J = 5.8 Hz, 2H, NHCH$_2$CH_2OH), 6.75 (d, J = 6.9 Hz, 1H, ArH), 7.69 (t, J = 8.0 Hz, 1H, ArH), 8.15 (d, J = 8.4 Hz, 1H, ArH), 8.50 (d, J = 7.2 Hz, 1H, ArH), 8.63 (d, J = 7.2 Hz, 1H, ArH); MS (EI) calcd for C$_{15}$H$_{13}$BrN$_2$O$_2$ [M]$^+$: 332.0, found: 332.0.

*4.1.4.2. 6-((2-Bromoethyl)amino)-2-ethy-1H-benzo[de]isoquinoline-1,3 (2H)-dione (**2c**).* Orange solid (80.2% yield); mp: 209.1–209.2 °C; ^{1}H NMR (400 MHz, CDCl$_3$): δ 1.32 (t, J = 7.2 Hz, 3H, CH$_2$CH_3), 3.76 (t, J = 6.0 Hz, 2H, NHCH_2CH$_2$OH), 3.87 (t, J = 6.0 Hz, 2H, NHCH$_2$CH_2OH), 4.23 (q, J = 7.2 Hz, 2H, CH_2CH$_3$), 6.75 (d, J = 8.4 Hz, 1H, ArH), 7.68 (t, J = 8.0 Hz, 1H, ArH), 8.14 (d, J = 8.4 Hz, 1H, ArH), 8.48 (d, J = 8.4 Hz, 1H, ArH), 8.61 (d, J = 7.2 Hz, 1H, ArH); ^{13}C NMR (100 MHz, CDCl$_3$): δ 13.4 (CH$_2$CH$_3$), 30.9 (NHCH$_2$CH$_2$Br), 35.3 (NHCH$_2$CH$_2$Br), 44.6 (CH$_2$CH$_3$), 104.6 (ArC), 111.8 (ArC), 120.6 (ArC), 123.4 (ArC), 125.8 (ArC), 129.7 (ArC), 131.2 (ArC), 134.0 (ArC), 148.2 (ArC), 163.9 (C=O, 164.4 (C=O); MS (ESI) calcd for C$_{16}$H$_{15}$BrN$_2$O$_2$ [M + H]$^+$: 347.0, found: 347.0.

*4.1.4.3. 6-((2-Bromoethyl)amino)-2-butyl-1H-benzo[de]isoquinoline-1,3 (2H)-dione (**4c**).* Orange solid (83.0% yield); mp: 155.0–156.0 °C; ^{1}H NMR (400 MHz, CDCl$_3$): δ 0.99 (t, J = 7.2 Hz, 3H, CH$_2$CH$_2$CH$_2$CH_3), 1.41–1.51 (m, 2H, CH$_2$CH$_2$CH_2CH$_3$), 1.69–1.77 (m, 2H, CH$_2$CH_2CH$_2$CH$_3$), 3.77 (t, J = 6.0 Hz, 2H, NHCH_2CH$_2$OH), 3.89 (t, J = 6.0 Hz, 2H, NHCH$_2$CH_2OH), 4.18 (t, J = 7.6 Hz, 2H, CH_2CH$_2$CH$_2$CH$_3$), 6.76 (d, J = 8.4 Hz, 1H, ArH), 7.68 (t, J = 8.0 Hz, 1H, ArH), 8.15 (d, J = 8.4 Hz, 1H, ArH), 8.49 (d, J = 8.4 Hz, 1H, ArH), 8.62 (d, J = 7.2 Hz, 1H, ArH); ^{13}C NMR (100 MHz, CDCl$_3$): δ 13.9 (C$_3$H$_6$CH$_3$), 20.4 (C$_2$H$_4$CH$_2$CH$_3$), 30.3 (CH$_2$CH$_2$C$_2$H$_5$), 30.9 (NHCH$_2$CH$_2$Br), 40.1 (NHCH$_2$CH$_2$Br), 44.6 (CH$_2$C$_3$H$_7$), 104.6 (ArC), 111.8 (ArC), 120.6 (ArC), 123.4 (ArC), 125.2 (ArC), 125.8 (ArC), 129.7 (ArC), 131.3 (ArC), 134.1 (ArC), 148.2 (ArC), 164.1 (C=O), 164.6 (C=O); MS (ESI) calcd for C$_{18}$H$_{20}$BrN$_2$O$_2$ [M + H]$^+$: 375.1, found: 375.0.

*4.1.4.4. 6-((2-Bromoethyl)amino)-2-hexyl-1H-benzo[de]isoquinoline-1,3 (2H)-dione (**6c**).* Orange solid (78.5% yield); mp: 148.2–148.7 °C; ^{1}H NMR (400 MHz, CDCl$_3$): δ 0.88 (t, J = 6.8 Hz, 3H, CH$_2$CH$_2$C$_3$H$_6$CH_3), 1.31–1.41 (m, 6H, CH$_2$CH$_2$C$_3H_6$CH$_3$), 1.67–1.75 (m, 2H, CH$_2$CH_2C$_3$H$_6$CH$_3$), 3.74 (t, J = 6.0 Hz, 2H, NHCH_2CH$_2$OH), 3.86 (t, J = 6.0 Hz, 2H, NHCH$_2$CH_2OH), 4.14 (t, J = 7.6 Hz, 2H, CH_2CH$_2$C$_3$H$_6$CH$_3$), 6.73 (d, J = 8.4 Hz, 1H, ArH), 7.64 (t, J = 7.6 Hz, 1H, ArH), 8.13 (d, J = 8.4 Hz, 1H, ArH), 8.45 (d, J = 8.4 Hz, 1H, ArH), 8.58 (d, J = 7.2 Hz, 1H, ArH); ^{13}C NMR (100 MHz, CDCl$_3$): δ 14.1 (C$_5$H$_{10}$CH$_3$), 22.6 (C$_4$H$_8$CH$_2$CH$_3$), 26.9 (C$_3$H$_6$CH$_2$C$_2$H$_5$), 28.2 (C$_2$H$_4$CH$_2$C$_3$H$_7$), 30.9 (CH$_2$CH$_2$C$_4$H$_9$), 31.6 (NHCH$_2$CH$_2$Br), 40.3 (NHCH$_2$CH$_2$Br), 44.7 (CH$_2$C$_5$H$_{11}$), 104.6 (ArC), 111.7 (ArC), 120.6 (ArC), 123.3 (ArC), 125.2 (ArC), 125.8 (ArC), 129.7 (ArC), 131.3 (ArC), 134.1 (ArC), 148.2 (ArC), 164.0 (C=O), 164.5 (C=O); MS (ESI) calcd for C$_{20}$H$_{24}$BrN$_2$O$_2$ [M + H]$^+$: 403.1, found: 403.1.

*4.1.4.5. 6-((2-Bromoethyl)amino)-2-cetyl-1H-benzo[de]isoquinoline-1,3 (2H)-dione (**16c**).* Orange solid (78.7% yield); mp: 121.6–121.9 °C; ^{1}H NMR (400 MHz, CDCl$_3$): δ 0.88 (t, J = 6.4 Hz, 3H, CH$_2$CH$_2$C$_{13}$H$_{26}$CH_3), 1.24–1.43 (m, 26H, CH$_2$CH$_2$C$_{13}H_{26}$CH$_3$), 1.68–1.75 (m, 2H, CH$_2$CH_2C$_{13}$H$_{26}$CH$_3$), 3.75 (t, J = 6.0 Hz, 2H, NHCH_2CH$_2$OH), 3.87 (t, J = 6.0 Hz, 2H, NHCH$_2$CH_2OH), 4.15 (t, J = 7.6 Hz, 2H, CH_2CH$_2$C$_{13}$H$_{26}$CH$_3$), 6.73 (d, J = 8.4 Hz, 1H, ArH), 7.65 (t, J = 7.6 Hz, 1H, ArH), 8.14 (d, J = 8.4 Hz, 1H, ArH), 8.46 (d, J = 8.4 Hz, 1H, ArH), 8.59 (d, J = 6.8 Hz, 1H, ArH); ^{13}C NMR (100 MHz, CDCl$_3$): δ 14.1 (C$_{15}$H$_{30}$CH$_3$), 22.7 (C$_{14}$H$_{28}$CH$_2$CH$_3$), 27.2 (C$_2$H$_4$C$_{12}$H$_{24}$C$_2$H$_5$), 28.2 (C$_2$H$_4$C$_{12}$H$_{24}$C$_2$H$_5$), 29.4 (C$_2$H$_4$C$_{12}$H$_{24}$C$_2$H$_5$), 29.4 (C$_2$H$_4$C$_{12}$H$_{24}$C$_2$H$_5$), 29.6 (C$_2$H$_4$C$_{12}$H$_{24}$C$_2$H$_5$), 29.7 (C$_2$H$_4$C$_{12}$H$_{24}$C$_2$H$_5$), 29.7 (C$_2$H$_4$C$_{12}$H$_{24}$C$_2$H$_5$), 30.8 (C$_2$H$_4$C$_{12}$H$_{24}$C$_2$H$_5$), 31.9 (NHCH$_2$CH$_2$Br), 40.3 (NHCH$_2$CH$_2$Br), 44.7 (CH$_2$C$_{15}$H$_{31}$), 104.5 (ArC), 111.6 (ArC), 120.5 (ArC), 123.3 (ArC), 124.1 (ArC), 125.8 (ArC), 129.7 (ArC), 131.2 (ArC), 134.0 (ArC), 148.3 (ArC), 164.0 (C=O), 164.5 (C=O); MS (ESI) calcd for C$_{30}$H$_{44}$BrN$_2$O$_2$ [M + H]$^+$: 543.2, found: 543.2.

*4.1.5. General procedure for the preparation of **1d–16d***

To a stirred solution of the bromide precursor (0.225 mmol) and KI (45 mg, 0.271 mmol) in dry CHCl$_3$ was added the N^1,N^1-dimethylethane-1,2-diamine (1.12 mmol) under argon. The mixture was heated and refluxed for 48 h. The reaction mixture was then cooled to room temperature and concentrated under vacuum.

*4.1.5.1. 6-((2-((2-(dimethylamino)ethyl)amino)ethyl)amino)-2-methyl-1H-benzo[de] isoquinoline-1,3(2H)-dione (**1d**).* The crude product was purified by column chromatography on silica gel (DCM:MeOH:Et$_3$N = 100:20:1, v/v/v) to provide **1d**. Orange solid (62.0% yield); mp: 93.4–94.7 °C; ^{1}H NMR (400 MHz, CD$_3$OD): δ 2.31 (s, 6H, N(CH_3)$_2$), 2.57 (t, J = 6.8 Hz, 2H, NCH$_2$CH$_2$NHCH$_2$CH_2N), 2.85 (t, J = 6.8 Hz, 2H, NCH$_2$CH$_2$NHCH_2CH$_2$N), 2.98 (t, J = 6.4 Hz, 2H, NCH$_2$CH_2NHCH$_2$CH$_2$N), 3.22 (s, 3H, CH_3), 3.42 (t, J = 6.4 Hz, 2H,

NC*H*$_2$CH$_2$NHCH$_2$CH$_2$N), 6.35 (d, J = 8.4 Hz, 1H, Ar*H*), 7.21 (t, J = 8.0 Hz, 1H, Ar*H*), 7.77 (d, J = 8.4 Hz, 1H, Ar*H*), 7.93 (d, J = 6.8 Hz, 1H, Ar*H*), 8.01 (d, J = 8.0 Hz, 1H, Ar*H*); ^{13}C NMR (100 MHz, CD$_3$OD): δ 25.6 (*C*H$_3$), 42.3 (NHCH$_2$CH$_2$N(*C*H$_3$)$_2$), 44.2 (NHCH$_2$CH$_2$N(CH$_3$)$_2$), 46.1 (NHCH$_2$*C*H$_2$NH), 48.5 (NH*C*H$_2$CH$_2$NH), 58.0 (NHCH$_2$*C*H$_2$N(CH$_3$)$_2$), 103.5 (Ar*C*), 108.1 (Ar*C*), 120.2 (Ar*C*), 121.5 (Ar*C*), 123.8 (Ar*C*), 127.6 (Ar*C*), 129.2 (Ar*C*), 130.4 (Ar*C*), 134.1 (Ar*C*), 150.7 (Ar*C*), 164.2 (*C*=O), 164.7 (*C*=O); HRMS (ESI) calcd for C$_{19}$H$_{25}$N$_4$O$_2$ [M + H]$^+$: 341.1978, found: 341.1974.

*4.1.5.2. 6-((2-((2-(dimethylamino)ethyl)amino)ethyl)amino)-2-ethyl-1H-benzo[de] isoquinoline-1,3(2H)-dione (**2d**).* The crude product was purified by column chromatography on silica gel (DCM:MeOH:Et$_3$N = 100:20:1, v/v/v) to provide **2d**. Orange solid (65.0% yield); mp: 93.0–94.1 °C; ^{1}H NMR (400 MHz, CD$_3$OD): δ 1.24 (t, J = 6.8 Hz, 3H, CH$_2$C*H*$_3$), 2.32 (s, 6H N(C*H*$_3$)$_2$), 2.59 (t, J = 6.8 Hz, 2H, NCH$_2$CH$_2$NHCH$_2$C*H*$_2$N), 2.86 (t, J = 6.8 Hz, 2H NCH$_2$CH$_2$NHC*H*$_2$CH$_2$N), 3.03 (t, J = 6.4 Hz, 2H NCH$_2$C*H*$_2$NHCH$_2$CH$_2$N), 3.51 (t, J = 6.4 Hz, 2H NC*H*$_2$CH$_2$NHCH$_2$CH$_2$N), 4.04 (q, J = 7.2 Hz, 2H, C*H*$_2$CH$_3$), 6.55 (d, J = 8.8 Hz, 1H, Ar*H*), 7.38 (t, J = 8.0 Hz, 1H, Ar*H*), 8.03 (d, J = 8.4 Hz, 1H, Ar*H*), 8.17 (d, J = 7.6 Hz, 1H, Ar*H*), 8.20 (d, J = 8.4 Hz, 1H, Ar*H*); ^{13}C NMR (100 MHz, CD$_3$OD): δ 13.75 (CH$_2$CH$_3$), 36.02 (*C*H$_2$CH$_3$), 43.59 (NHCH$_2$CH$_2$N(CH$_3$)$_2$), 45.59 (NHCH$_2$CH$_2$N(*C*H$_3$)$_2$), 47.4 (NHCH$_2$*C*H$_2$NH), 48.5 (NH*C*H$_2$CH$_2$NH), 59.3 (NHCH$_2$*C*H$_2$N(CH$_3$)$_2$), 104.9 (Ar*C*), 109.6 (Ar*C*), 121 (Ar*C*), 123.0 (Ar*C*), 125.2 (Ar*C*), 128.9 (Ar*C*), 130.6 (Ar*C*), 131.7 (Ar*C*), 135.3 (Ar*C*), 152.0 (Ar*C*), 165.1 (*C*=O), 165.60 (*C*=O); HRMS (ESI) calcd for C$_{20}$H$_{27}$N$_4$O$_2$ [M + H]$^+$: 355.2134, found: 355.2134.

*4.1.5.3. 6-((2-((2-(dimethylamino)ethyl)amino)ethyl)amino)-2-butyl-1H-benzo[de] isoquinoline-1,3(2H)-dione (**4d**).* The crude product was purified by column chromatography on silica gel (DCM:MeOH:Et$_3$N = 100:15:1, v/v/v) to provide 4d. Orange solid (67.0% yield); mp: 90.1–92.0 °C; ^{1}H NMR (400 MHz, CDCl$_3$): δ 0.97 (t, J = 7.2 Hz, 3H, CH$_2$CH$_2$CH$_2$C*H*$_3$), 1.40–1.49 (m, 2H, CH$_2$CH$_2$C*H*$_2$CH$_3$), 1.67–1.75 (m, 2H, CH$_2$*CH*$_2$CH$_2$CH$_3$), 2.27 (s, 6H, N(CH$_3$)$_2$), 2.49 (t, J = 6.0 Hz, 2H, NCH$_2$CH$_2$NCH$_2$C*H*$_2$N), 2.78 (t, J = 6.0 Hz, 2H, NCH$_2$CH$_2$NC*H*$_2$CH$_2$N), 3.10 (t, J = 5.6 Hz, 2H, NCH$_2$C*H*$_2$NCH$_2$CH$_2$N), 3.43 (q, J = 5.2 Hz, 2H, NC*H*$_2$CH$_2$NCH$_2$CH$_2$N), 4.16 (t, J = 7.6 Hz, 2H, C*H*$_2$CH$_2$CH$_2$CH$_3$), 6.43 (s, 1H, Ar*H*), 6.67 (d, J = 8.4 Hz, 1H, Ar*H*), 7.60 (t, J = 7.8 Hz, 1H, Ar*H*), 8.22 (d, J = 8.4 Hz, 1H, Ar*H*), 8.44 (d, J = 8.4 Hz, 1H, Ar*H*), 8.57 (d, J = 7.2 Hz, 1H, Ar*H*); ^{13}C NMR (100 MHz, CDCl$_3$): δ 13.9 (C$_3$H$_7$CH$_3$), 20.5 (C$_2$H$_4$*C*H$_2$CH$_3$), 30.3 (CH$_2$CH$_2$C$_2$H$_5$), 40.0 (*C*H$_2$C$_3$H$_7$), 42.2 (NHCH$_2$CH$_2$N(CH$_3$)$_2$), 45.4 (NHCH$_2$CH$_2$N(*C*H$_3$)$_2$), 46.3 (NHCH$_2$*C*H$_2$NH), 47.3 (NH*C*H$_2$CH$_2$NH), 58.8 (NHCH$_2$*C*H$_2$N(CH$_3$)$_2$), 104.3, 110.1, 120.5, 123.0, 124.6, 126.6, 129.8, 131.1, 134.5, 149.7, 164.2, 164.8; HRMS (ESI) calcd for C$_{22}$H$_{31}$N$_4$O$_2$ [M + H]$^+$: 383.2447, found: 383.2445.

*4.1.5.4. 6-((2-((2-(dimethylamino)ethyl)amino)ethyl)amino)-2-hexyl-1H-benzo[de] isoquinoline-1,3(2H)-dione (**6d**).* The resulting mixture was diluted with water (10 mL) containing 10% NaCl and 1% Na$_2$CO$_3$ and extracted with CH$_2$Cl$_2$ (3 × 15 mL). The organic layer was then concentrated under vacuum and then further purified. The crude product was purified by column chromatography on silica gel (DCM:MeOH:Et$_3$N = 100:10:1, v/v/v) to provide **6d**. Orange solid (71.0% yield); mp: 83.2–85.1 °C; ^{1}H NMR (400 MHz, CDCl$_3$): δ 0.88 (t, J = 6.8 Hz, 3H, CH$_2$CH$_2$C$_3$H$_6$C*H*$_3$), 1.31–1.42 (m, 6H, CH$_2$CH$_2$C$_3$*H*$_6$CH$_3$), 1.70–1.72 (m, 2H, CH$_2$*CH*$_2$C$_3$H$_6$CH$_3$), 2.27 (s, 6H, N(*CH*$_3$)$_2$), 2.51 (t, J = 6.4 Hz, 2H, NCH$_2$CH$_2$NCH$_2$C*H*$_2$N), 2.80 (t, J = 6.0 Hz, 2H, NCH$_2$CH$_2$NC*H*$_2$CH$_2$N), 3.11 (t, J = 6.0 Hz, 2H, NCH$_2$C*H*$_2$NCH$_2$CH$_2$N), 3.44 (t, J = 6.0 Hz, 2H, NC*H*$_2$CH$_2$NCH$_2$CH$_2$N), 4.14 (t, J = 7.6 Hz, 2H, C*H*$_2$CH$_2$C$_3$H$_6$CH$_3$), 6.49 (s, 1H, Ar*H*), 6.65 (d, J = 8.4 Hz, 1H, Ar*H*), 7.59 (t, J = 8.0 Hz, 1H, Ar*H*), 8.25 (d, J = 8.0 Hz, 1H, Ar*H*), 8.42 (d, J = 8.4 Hz, 1H, Ar*H*), 8.55 (d, J = 7.2 Hz, 1H, Ar*H*); ^{13}C NMR (100 MHz, CDCl$_3$): δ 14.1 (C$_5$H$_{10}$*C*H$_3$), 22.6 (C$_4$H$_{10}$*C*H$_2$CH$_3$), 26.9 (C$_3$H$_6$*C*H$_2$C$_2$H$_5$), 28.2 (C$_2$H$_4$*C*H$_2$C$_3$H$_7$), 31.6 (CH$_2$*C*H$_2$C$_4$H$_9$), 40.2 (*C*H$_2$C$_5$H$_{11}$), 42.2 (NHCH$_2$CH$_2$N(CH$_3$)$_2$), 45.4 (NHCH$_2$CH$_2$N(*C*H$_3$)$_2$), 46.2 (NHCH$_2$*C*H$_2$NH), 47.3 (NHCH$_2$CH$_2$NH), 58.6 (NHCH$_2$*C*H$_2$N(CH$_3$)$_2$), 104.3 (Ar*C*), 110.1 (Ar*C*), 120.5 (Ar*C*), 123.0 (Ar*C*), 124.5 (Ar*C*), 126.7 (Ar*C*), 129.8 (Ar*C*), 131.0 (Ar*C*), 134.5 (Ar*C*), 149.8 (Ar*C*), 164.2 (*C*=O), 164.7 (*C*=O); HRMS (ESI) calcd for C$_{24}$H$_{35}$N$_4$O$_2$ [M + H]$^+$: 411.2760, found: 411.2755.

*4.1.5.5. 6-((2-((2-(dimethylamino)ethyl)amino)ethyl)amino)-2-cetyl-1H-benzo[de] isoquinoline-1,3(2H)-dione (**16d**).* The resulting mixture was diluted with water (10 mL) containing 10% NaCl and 1% Na$_2$CO$_3$ and extracted with CH$_2$Cl$_2$ (3 × 15 mL). The organic layer was then concentrated under vacuum and then further purified. The crude product was purified by column chromatography on silica gel (DCM:MeOH:Et$_3$N = 100:10:1, v/v/v) to provide **16d**. Orange solid (70.0% yield); mp: 128.6–130.2 °C; ^{1}H NMR (400 MHz, CDCl$_3$): δ 0.88 (t, J = 6.4 Hz, 3H, CH$_2$CH$_2$C$_{13}$H$_{26}$C*H*$_3$), 1.30–1.43 (m, 26H, CH$_2$CH$_2$C$_{13}$*H*$_{26}$CH$_3$), 1.67–1.74 (m, 2H, CH$_2$C*H*$_2$C$_{13}$H$_{26}$CH$_3$), 2.36 (s, 6H), 2.70 (t, J = 6.0 Hz, 2H, NCH$_2$CH$_2$NCH$_2$C*H*$_2$N), 2.92 (t, J = 6.0 Hz, 2H, NCH$_2$CH$_2$NC*H*$_2$CH$_2$N), 3.18 (t, J = 5.6 Hz, 2H, NCH$_2$C*H*$_2$NCH$_2$CH$_2$N), 3.59 (br, 2H, NC*H*$_2$CH$_2$NCH$_2$CH$_2$N), 4.13 (t, J = 7.6 Hz, 2H, C*H*$_2$CH$_2$C$_{13}$H$_{26}$CH$_3$), 6.63 (d, J = 8.4 Hz, 1H, Ar*H*), 6.93 (s, 1H, Ar*H*), 7.61 (t, J = 7.6 Hz, 1H, Ar*H*), 8.40 (d, J = 8.4 Hz, 1H, Ar*H*), 8.53–8.57 (m, 2H, Ar*H*); ^{13}C NMR (100 MHz, CDCl$_3$): δ 14.1 (C$_{15}$H$_{33}$CH$_3$), 22.7 (C$_{14}$H$_{28}$CH$_2$CH$_3$), 27.3 (C$_2$H$_4$C$_{12}$H$_{24}$C$_2$H$_5$), 28.3 (C$_2$H$_4$C$_{12}$H$_{24}$C$_2$H$_5$), 29.4 (C$_2$H$_4$C$_{12}$H$_{24}$C$_2$H$_5$), 29.5 (C$_2$H$_4$C$_{12}$H$_{24}$C$_2$H$_5$), 29.6 (C$_2$H$_4$C$_{12}$H$_{24}$C$_2$H$_5$), 29.7 (C$_2$H$_4$C$_{12}$H$_{24}$C$_2$H$_5$), 29.7 (C$_2$H$_4$C$_{12}$H$_{24}$C$_2$H$_5$), 31.9 (CH$_2$CH$_2$C$_{14}$H$_{29}$), 40.2 (*C*H$_2$C$_{15}$H$_{31}$), 41.9 (NHCH$_2$CH$_2$N(CH$_3$)$_2$), 44.8 (NHCH$_2$CH$_2$N(CH$_3$)$_2$), 45.4 (NHCH$_2$*C*H$_2$NH), 47.0 (NHCH$_2$CH$_2$NH), 57.4 (NHCH$_2$*C*H$_2$N(CH$_3$)$_2$), 104.9 (Ar*C*), 110.2 (Ar*C*), 120.7 (Ar*C*), 122.8 (Ar*C*), 124.7 (Ar*C*), 127.7 (Ar*C*), 129.8 (Ar*C*), 131.2 (Ar*C*), 134.3 (Ar*C*), 149.7 (Ar*C*), 164.2(*C*=O), 164.8 (*C*=O); HRMS (ESI) calcd for C$_{34}$H$_{55}$N$_4$O$_2$ [M + H]$^+$: 551.4325, found: 551.4329.

4.2. kDNA decatenation assay [29]

Topo II activity was measured by the ATP-dependent decatenation of kinetoplast DNA (kDNA) according to the manufacturer's instructions (TopoGEN, Florida, USA). 0.1 μg kDNA, 1 unit of human topoIIα (TopoGEN) and the indicated concentrations of compounds were incubated for 30 min at 37 °C in 50 mM Tris–HCl (pH 8.0), 150 mM NaCl, 10 mM MgCl$_2$, 2 mM ATP, 0.5 mM DTT in a total volume of 20 μL. The reactions were stopped by the addition of 2 μL 10% SDS and 2 μL 6× loading dye solution (Fermentas). Samples were then electrophoresed in 0.8% agarose gel in TAE buffer for 50 min at 120 V. The gel was stained with ethidium bromide at room temperature and photographed with UV transilluminator.

4.3. DNA intercalating assay by CD spectra

ct-DNA was purchased from Sigma Aldrich and used without further purification. A solution of ct-DNA in 20 mM Tris-HCl buffer (pH = 7.4) was stored at 4 °C. The concentration of ct-DNA was determined spectrophotometrically from themolar absorption coefficient (6600 M^{-1} cm^{-1}). The stock solution was attested to be sufficiently free from protein, as it gave a UV absorbance ratio at 260 and 280 nm of more than 1.8. The CD measurements were performed on a Chirascan spectrophotometer (Photophysics, England) using 1 cm quartz cell in the range of 200–400 nm ct-DNA (100 μM) interacted with drugs (20 μM) in Tris-HCl buffer for 2 h at 25 °C. CD spectra in the range of 230–300 nm were analyzed.

4.4. DNA intercalating assay by fluorescence spectra [34]

The fluorescence spectra were obtained using a Varian Cary Eclipse fluorescence spectrophotometer at 25 °C. The concentrations of compounds and calf thymus DNA were 10 μM and 0–80 μM respectively in 20 mM Tris-HCl buffer (pH = 7.5) and 1% DMSO. And an equilibrium period of 1 h for constant stirring at 25 °C in the dark was allowed. The association constants (Kb) were derived according to equation $I = I_0+\{(I_\infty - I_0)/2[Q]_0)\} \times \{([DNA]_0+[Q]_0 + 1/Ka) - \{([DNA]_0+[Q]_0 + 1/Ka)^2 - 4[DNA]_0[Q]_0\}^{1/2}\}$, wherein I_0, I and I_∞ represent the fluorescence intensities of compounds alone, the sample and DNA totally bound, respectively. $[DNA]_0$ and $[Q]_0$ were the initial analytical concentrations of DNA and the agents, respectively.

4.5. Evaluation of solubility [35] and logP

A Varian Cary100 Bio UV–Visible spectrophotometer was used to detect the absorption spectra of the tested compounds. Stock solutions of the tested compounds were prepared in DMSO at a concentration of 10^{-3} M. The maximum absorbance wavelengths of the compounds were all around 450 nm. Standard curves of the compounds were tested by several concentrations in PBS (20 mM, pH = 7.4). The equations obtained from the standard curves were used to calculate the corresponding solubility. In detail, excessive compound was added to PBS, and shaken for 24 h to be fully dissolved. The mixture was centrifugated at 10^4 rpm for 10 min. Then the saturated supernatant was taken for detection. The supernatant was diluted to the concentration range of corresponding standard curve. The solubility was calculated by the equation of standard curve from three independent tests. The log *P* values were calculated with ACD/Labs software V12.

4.6. Cell lines and cell culture

MDA-MB-231, A549, HMEC-1 were purchased from American Type Culture Collection (ATCC, Manassas, VA, USA). HL60 and LO2 were from Shanghai Institute of Biochemistry and Cell Biology (Shanghai, China). GES-1 was obtained from Renji Hospital (Shanghai, China). They were maintained in strict accordance with the supplier's instructions and established procedures.

4.7. Cell proliferation assay

Cell proliferation was evaluated using the SRB or MTT assay. Firstly, cancer cells were seeded into 96-well plates and cultured overnight. The cells were then treated with increasing concentrations of compounds for a further 72 h. For MDA-MB-231, A549, LO2, GES-1, HMEC-1 cell lines, cells were then fixed with 10% trichloroacetic acid and stained with sulforhodamine B (Sigma). Sulforhodamine B in the cells was dissolved in 10 mM Tris–HCl and was measured at 515 nm using a multiwell spectrophotometer (MAX190™, Molecular Devices, Sunnyvale, USA). The inhibition rate on cell proliferation was calculated as follows: inhibition rate = $(1 - A_{515\ treated}/A_{515\ control}) \times 100\%$. For HL60 cell line, 20 μL (5 mg/mL in 0.9% brine) of MTT (Sigma) was added to each well. The cells were then incubated for an additional 4 h, after which 100 μL of "triplex solution" (10% SDS-5% isobutanol-HCl, 12 mM) was added, and the cells were incubated overnight at 37 °C. The plates were read at 570 nm on the scanning multiwell spectrophotometer (MAX190™). The inhibition rate on cell proliferation was calculated as: inhibition rate = $(1 - A_{570\ treated}/A_{570\ control}) \times 100\%$. The IC_{50} values were obtained by the Logit method. Each experiment was repeated in triplicate.

4.8. Protein kinase assays [36]

Tyrosine kinase activity was determined by an enzyme-linked-immunosorbent assay (ELISA) in 96-well plates pre-coated with 2.5 μg/well poly $(Glu, Tyr)_{4:1}$ (Sigma) as a substrate. Fifty microliters of 10 μM ATP solution diluted in reaction buffer [50 mM HEPES, pH 7.4, 20 mM $MgCl_2$, 0.1 mM Na_3VO_4, and 1 mM DTT] was added to each well, and the reaction was initiated by the addition of increasing concentrations of tyrosine kinase. After incubation for 1 h at 37 °C, the plate was washed three times with phosphate buffered saline containing 0.1% Tween20 (PBST). Next, 100 μL of antiphosphotyrosine (PY99; 1:1000 dilution) antibody was added. After 0.5 h incubation at 37 °C, the plate was washed three times and goat anti-mouse IgG horseradish peroxidase (100 μL of a 1:2000 dilution) diluted in PBST containing 5 mg/mL BSA was added. The plate was reincubated at 37 °C for 0.5 h and washed as before. Finally, 100 μL of color development solution (0.03% H_2O_2 and 2 mg/mL *o*-phenylenediamine in 0.1 M citrate buffer, pH 5.4) was added and the plate was incubated at room temperature until color emerged. The reaction was terminated by the addition of 50 μL of 2 M H_2SO_4, and then the plate was read using a multi-well spectrophotometer (MAX190™) at 490 nm. The inhibition rate (%) was calculated using the following equation: inhibition rate = $[1 - (A_{490\ treated}/A_{490control})] \times 100\%$. IC_{50} values were determined from the results of at least three independent tests and calculated from the inhibition curves.

4.9. Cell migration assay

HMEC-1s migration was determined in a transwell Boyden chamber (Costar, MA, USA) [37]. Briefly, cell suspension (5×10^5 cells/mL) with different concentrations of **8d** or control was added to the upper compartment of the chamber. The lower compartment contained 20% FBS MCDB131 medium and the same concentrations of **8d** or control. After incubation (6 h, 37 °C), the inhibition of migration was calculated: inhibition of migration = $[1 - (A_{compound} - A_{blank})/(A_{control} - A_{blank})] \times 100\%$.

4.10. Tube formation assay

Matrigel (75 mL $well^{-1}$) was used to coat 96-well plates, allowed to solidify (37 °C, 1 h) [38], prior to seeding with HMEC-1s (1×10^5 cells/mL) that were then cultured (37 °C, 8 h) in MCDB131 medium with 20% FBS containing **8d** or control. For investigation of neovessel disruption, HMEC-1s were seeded on Matrigel and left to align for 24 h. The formed capillary-like structures or cords were exposed to **8d**, and then examined with an inverted phase contrast microscope (DP70, Olympus, Japan). The number of the tubes was quantified from five random fields. The inhibition of tube formation was calculated: inhibition of tube formation = $[1 - (tubes_{compound}/tubes_{control})] \times 100\%$.

4.11. Western blot analysis [39]

HMEC-1 cells were plated into 6-well plate (3×10^5 cell/well). After adherence, cells were starved and incubated in serum-free medium for 24 h and then exposed to corresponding compounds for 12 h. For analysis of FGFR1 phosphorylation and downstream signal transduction pathways, cells were stimulated with 50 ng/ml bFGF for 10 min at 37 °C at the end of compounds treatment. Whole-cell lysates were collected and boiled for 10 min in 2 × SDS sample buffer, subjected to 10% SDS-PAGE, and transferred to nitrocellulose (Amersham Life Sciences). The blot was blocked in blocking buffer (5% non-fat dry milk/1% Tween-20 in TBS) for 1 h at room temperature, and then incubated with primary antibodies

(anti- phospho-FGFR1 (1:200), anti-phospho-AKT (1:500), anti-phospho-Erk (1:2000) and anti-GAPDH (1:10000)) in blocking buffer for 2 h at room temperature. The bands were then visualized using horseradish peroxidase-conjugated secondary antibodies (1:2000) followed by ECL (Pierce Biotech, Rockford, IL).

Acknowledgments

This work is financially supported by the National Basic Research Program of China (973 Program, 2010CB126100), the National High Technology Research and Development Program of China (863 Program 2011AA10A207), the National Natural Science Foundation of China (Grant 81173080), the Shanghai Committee of Science and Technology (Grant 10431902600 and Grant 11DZ2260600), the Fundamental Research Funds for the Central Universities.

Appendix A. Supplementary data

Supplementary data related to this article can be found at http://dx.doi.org/10.1016/j.ejmech.2013.05.002.

References

[1] G.I. Giles, R.P. Sharma, Topoisomerase enzymes as therapeutic targets for cancer chemotherapy, Med. Chem. 1 (2005) 383–394.
[2] J.A.W. Byl, S.D. Cline, T. Utsugi, T. Kobunai, Y. Yamada, N. Osheroff, DNA topoisomerase II as the target for the anticancer drug TOP-53: mechanistic basis for drug action, Biochemistry 40 (2001) 712–718.
[3] K. Chikamori, A.G. Grozav, T. Kozuki, D. Grabowski, R. Ganapathi, M.K. Ganapathi, DNA topoisomerase II enzymes as molecular targets for cancer chemotherapy, Curr. Cancer Drug Targets 10 (2010) 758–771.
[4] L.H. Hurley, DNA and its associated processes as targets for cancer therapy, Nat. Rev. Cancer 2 (2002) 188–200.
[5] M.A. Lemmon, J. Schlessinger, Cell signaling by receptor tyrosine kinases, Cell 141 (2010) 1117–1134.
[6] Z. Fu, L. Malureanu, J. Huang, W. Wang, H. Li, J.M. van Deursen, D.J. Tindall, J. Chen, Plk1-dependent phosphorylation of FoxM1 regulates a transcriptional programme required for mitotic progression, Nat. Cell. Biol. 10 (2008) 1076–1082.
[7] K. Gotink, H. Verheul, Anti-angiogenic tyrosine kinase inhibitors: what is their mechanism of action? Angiogenesis 13 (2010) 1–14.
[8] J. Drevs, M. Medinger, C. Schmidt-Gersbach, R. Weber, C. Unger, Receptor tyrosine kinases: the main targets for new anticancer therapy, Curr. Drug Targets 4 (2003) 113–121.
[9] N. Ferrara, R.S. Kerbel, Angiogenesis as a therapeutic target, Nature 438 (2005) 967–974.
[10] M. Tsanakopoulou, T. Cottin, A. Buttner, V. Sarli, E. Malamidou-Xenikaki, S. Spyroudis, A. Giannis, Indeno[1,2-d]pyrido[1,2-a]pyrimidines: a new class of receptor tyrosine kinase inhibitors, Chemmedchem 3 (2008) 429–433.
[11] S.K. Jung, K.W. Lee, S. Byun, E.J. Lee, J.E. Kim, A.M. Bode, Z. Dong, H.J. Lee, Myricetin inhibits UVB-induced angiogenesis by regulating PI-3 kinase in vivo, Carcinogenesis 31 (2010) 911–917.
[12] M. Presta, P. Dell'Era, S. Mitola, E. Moroni, R. Ronca, M. Rusnati, Fibroblast growth factor/fibroblast growth factor receptor system in angiogenesis, Cytokine Growth Factor Rev. 16 (2005) 159–178.
[13] L.Q. Chow, S.G. Eckhardt, Sunitinib: from rational design to clinical efficacy, J. Clin. Oncol. 25 (2007) 884–896.
[14] A. Gangjee, N. Zaware, S. Raghavan, M. Ihnat, S. Shenoy, R.L. Kisliuk, Single agents with designed combination chemotherapy potential: synthesis and evaluation of substituted pyrimido[4,5-b]indoles as receptor tyrosine kinase and thymidylate synthase inhibitors and as antitumor agents, J. Med. Chem. 53 (2010) 1563–1578.
[15] Z.F. Tao, L. Wang, K.D. Stewart, Z. Chen, W. Gu, M.H. Bui, P. Merta, H. Zhang, P. Kovar, E. Johnson, C. Park, R. Judge, S. Rosenberg, T. Sowin, N.H. Lin, Structure-based design, synthesis, and biological evaluation of potent and selective macrocyclic checkpoint kinase 1 inhibitors, J. Med. Chem. 50 (2007) 1514–1527.
[16] Z.W. Cai, Y. Zhang, R.M. Borzilleri, L. Qian, S. Barbosa, D. Wei, X. Zheng, L. Wu, J. Fan, Z. Shi, B.S. Wautlet, S. Mortillo, R. Jeyaseelan, D.W. Kukral, A. Kamath, P. Marathe, C. D'Arienzo, G. Derbin, J.C. Barrish, J.A. Robl, J.T. Hunt, L.J. Lombardo, J. Fargnoli, R.S. Bhide, Discovery of brivanib alaninate ((S)-((R)-1-(4-(4-fluoro-2-methyl-1H-indol-5-yloxy)-5-methylpyrrolo[2,1-f][1,2,4]triazin-6-yloxy)propan-2-yl)2-aminopropanoate), a novel prodrug of dual vascular endothelial growth factor receptor-2 and fibroblast growth factor receptor-1 kinase inhibitor (BMS-540215), J. Med. Chem. 51 (2008) 1976–1980.
[17] J. Ma, D.J. Waxman, Combination of antiangiogenesis with chemotherapy for more effective cancer treatment, Mol. Cancer Ther. 7 (2008) 3670–3684.
[18] A.A. Borisy, P.J. Elliott, N.W. Hurst, M.S. Lee, J. Lehar, E.R. Price, G. Serbedzija, G.R. Zimmermann, M.A. Foley, B.R. Stockwell, C.T. Keith, Systematic discovery of multicomponent therapeutics, Proc. Natl. Acad. Sci. U. S. A 100 (2003) 7977–7982.
[19] M.F. Braña, A. Ramos, Naphthalimides as anticancer agents: synthesis and biological activity, Curr. Med. Chem. – Anti-cancer Agents 1 (2001) 237–255.
[20] L. Ingrassia, F. Lefranc, R. Kiss, T. Mijatovic, Naphthalimides and azonafides as promising anti-cancer agents, Curr. Med. Chem. 16 (2009) 1192–1213.
[21] T. Mijatovic, T. Mahieu, N. De Neve, J. Dewelle, G. Simon, M.J.M. Dehoux, E. van der Aar, B. Haibe-Kains, G. Bontempi, C. Deacestecker, E. Van Quaquebeke, F. Darro, R. Kiss, UNBS5162, a novel naphthalimide that decreases CXCL chemokine expression in experimental prostate cancers, Neoplasia 10 (2008) 573–586.
[22] J.G. Kuhn, H.A. Burris, S.F. Jones, D.W. Hein, N.T. Willcutt, F.A. Greco, D.S. Thompson, A.A. Meluch, R.S. Schwartz, D.M. Brown, Phase I/II dose-escalation trial of amonafide for treatment of advanced solid tumors: genotyping to optimize dose based on polymorphic metabolism, J. Clin. Oncol. 25 (2007) 2503.
[23] A. Wu, Y. Xu, X. Qian, J. Wang, J. Liu, Novel naphthalimide derivatives as potential apoptosis-inducing agents: design, synthesis and biological evaluation, Eur. J. Med. Chem. 44 (2009) 4674–4680.
[24] M. Lv, H. Xu, Overview of naphthalimide analogs as anticancer agents, Curr. Med. Chem. 16 (2009) 4797–4813.
[25] Z. Chen, X. Liang, H.Y. Zhang, H. Xie, J.W. Liu, Y.F. Xu, W.P. Zhu, Y. Wang, X. Wang, S.Y. Tan, D. Kuang, X.H. Qian, A new class of naphthalimide-based antitumor agents that inhibit topoisomerase II and induce lysosomal membrane permeabilization and apoptosis, J. Med. Chem. 53 (2010) 2589–2600.
[26] N. Iranpoor, H. Firouzabadi, G. Aghapour, A.R. Vaezzadeh, Triphenylphosphine/2,3-dichloro-5,6-dicyanobenzoquinone as a new, selective and neutral system for the facile conversion of alcohols, thiols and selenols to alkyl halides in the presence of halide ions, Tetrahedron 58 (2002) 8689–8693.
[27] M.F. Brana, M. Cacho, A. Gradillas, B. de Pascual-Teresa, A. Ramos, Intercalators as anticancer drugs, Curr. Pharm. Des. 7 (2001) 1745–1780.
[28] H. Zhu, M. Huang, F. Yang, Y. Chen, Z.H. Miao, X.H. Qian, Y.F. Xu, Y.X. Qin, H.B. Luo, X. Shen, M.Y. Geng, Y.J. Cai, J. Ding, R16, a novel amonafide analogue, induces apoptosis and G(2)-M arrest via poisoning topoisomerase II, Mol. Cancer Ther. 6 (2007) 484–495.
[29] K. Tanabe, Y. Ikegami, R. Ishida, T. Andoh, Inhibition of topoisomerase-II by antitumor agents bis(2,6-dioxopiperazine) derivatives, Cancer Res. 51 (1991) 4903–4908.
[30] Z.Y. Tian, S.Q. Xie, Z.H. Mei, J. Zhao, W.Y. Gao, C.J. Wang, Conjugation of substituted naphthalimides to polyamines as cytotoxic agents targeting the Akt/mTOR signal pathway, Org. Biomol. Chem. 7 (2009) 4651–4660.
[31] S.Q. Xie, Q. Li, Y.H. Zhang, J.H. Wang, J. Zhao, C.J. Wang, NNINspm, naphthalimide-polyamine conjugate, induces hepatoma HepG2 cell apoptosis via PI3K/Akt pathways, Chin. Pharm. Bull. 26 (2010) 169–174.
[32] J. Marx, Angiogenesis: a boost for tumor starvation, Science 301 (2003) 452–454.
[33] C.J. Powers, S.W. McLeskey, A. Wellstein, Fibroblast growth factors, their receptors and signaling, Endocr. Relat. Cancer 7 (2000) 165–197.
[34] S. Tan, H. Yin, Z. Chen, X. Qian, Y. Xu, Oxo-heterocyclic fused naphthalimides as antitumor agents: synthesis and biological evaluation, Eur. J. Med. Chem. 62 (2013) 130–138.
[35] J. Alsenz, M. Kansy, High throughput solubility measurement in drug discovery and development, Adv. Drug Delivery Rev. 59 (2007) 546–567.
[36] L.J. Tong, H. Xie, T. Peng, X.F. Liu, X.L. Xin, X. Huang, S.M. Chen, H.Y. Liu, H.L. Li, M.Y. Geng, M. Yin, J. Ding, Establishment of platform for screening insulin-like growth factor-1 receptor inhibitors and evaluation of novel inhibitors, Acta Pharmacol Sin 32 (2011) 930–938.
[37] K.L. Osusky, D.E. Hallahan, A. Fu, F. Ye, Y. Shyr, L. Geng, The receptor tyrosine kinase inhibitor SU11248 impedes endothelial cell migration, tubule formation, and blood vessel formation in vivo, but has little effect on existing tumor vessels, Angiogenesis 7 (2004) 225–233.
[38] A. Kruczynski, M. Poli, R. Dossi, E. Chazottes, G. Berrichon, C. Ricome, R. Giavazzi, B.T. Hill, G. Taraboletti, Anti-angiogenic, vascular-disrupting and anti-metastatic activities of vinflunine, the latest vinca alkaloid in clinical development, Eur. J. Cancer 42 (2006) 2821–2832.
[39] H. Xie, L. Lin, L. Tong, Y. Jiang, M. Zheng, Z. Chen, X. Jiang, X. Zhang, X. Ren, W. Qu, Y. Yang, H. Wan, Y. Chen, J. Zuo, H. Jiang, M. Geng, J. Ding, AST1306, a novel irreversible inhibitor of the epidermal growth factor receptor 1 and 2, exhibits antitumor activity both in vitro and in vivo, PLoS One 6 (2011) e21487.